Koshland, D. E., & Neet, K. E. (1968) *Annu. Rev. Biochem. 37*, 359–410.
Liljas, A., & Rossmann, M. G. (1974) *Annu. Rev. Biochem. 44*, 475–507.
Porter, R. R. (1959) *Biochem. J. 73*, 119–126.
Rudolph, R., Heider, I., Westhof, E., & Jaenicke, R. (1977) *Biochemistry 16*, 3384–3390.
Schulz, G. E., & Shirmer, R. H. (1979) in *Principles of Protein Structure*, pp 66–107, Springer-Verlag, New York.
Setlow, P., & Kornberg, A. (1972) *J. Biol. Chem. 247*, 232–240.
Sibilli, L., Cossart, P., Chalvignac, M. A., Briley, P. A., Costrejean, J. M., Le Bras, G., & Cohen, G. N. (1977) *Biochimie 59*, 943–946.
Teipel, J. W., & Koshland, D. E. (1971) *Biochemistry 10*, 792–798.
Truffa-Bachi, P., & Cohen, G. N. (1970) *Methods Enzymol. 17A*, 694–699.
Truffa-Bachi, P., Vêron, M., & Cohen, G. N. (1974) CRC *Crit. Rev. Biochem. 2*, 379–415.
Vêron, M., Falcoz-Kelly, F., & Cohen, G. N. (1972) *Eur. J. Biochem. 28*, 520–527.
Vêron, M., Saari, J. C., Villar-Palasi, C., & Cohen, G. N. (1973) *Eur. J. Biochem. 38*, 325–335.
Wampler, E. D., & Westhead, E. W. (1968) *Biochemistry 7*, 1661–1671.

α-Chymotrypsin Deacylation: Temperature Dependence of Hydrolysis and Transesterification Reactions†

Chih-Lueh A. Wang, K. C. Calvo, and Michael H. Klapper*

ABSTRACT: The hydrolysis and transesterification reactions of furoyl-chymotrypsins display nonlinear Arrhenius plots with no apparent discontinuities. Of a number of models considered, the best explanation assumes a temperature-dependent rapid equilibrium between two forms of acyl-enzyme with differing reactivities. Rate constants for the transesterification of α-chymotrypsinyl 2-(5-*n*-propyl)furoate, after normalization for this equilibrium, display a linear free energy correlation with the Taft polarity constants σ* and volumes of the attacking alcohols.

Chymotrypsin catalyzes the hydrolysis, alcoholysis, and aminolysis of a large variety of esters and amides, and the literature describing these various reactions is extensive. It is not generally appreciated, although well documented, that the temperature dependence of many chymotrypsin-catalyzed reactions is not simple, as indicated by nonlinear Arrhenius plots [Baggott & Klapper (1976) and references therein]. Nor is a complicated temperature dependence unique to this enzyme; other examples are urease (Kistiakowsky & Lumry, 1949), the citrate-condensing enzyme (Kosicki & Srere, 1961), glycogen phosphorylase (Helmrich & Cori, 1964; Graves et al., 1965), pyruvate kinase (Kayne & Suelter, 1965), D-amino acid oxidase (Massey et al., 1966), lysozyme (Saint-Blancard et al., 1977), and ribonuclease (Matheson & Scheraga, 1979). Such nonlinearity may be more common than suggested by this short list, since reliable temperature dependencies have not been reported for many enzymes.

There are four general explanations for a nonlinear Arrhenius plot: (i) the activation enthalpy is temperature dependent; (ii) the reaction proceeds through at least two parallel paths to the same product (i.e., different reaction mechanisms are possible), with pathway predominance dependent on temperature; (iii) there is one (or more) kinetically significant reaction intermediate with a temperature-dependent shift in rate-limiting step; or (iv) there is a temperature-dependent equilibrium between enzyme forms which differ in catalytic efficiency. Since each of these general explanations may subsume two or more specific reaction mechanisms, or a combination from these four possibilities may be involved, a nonlinear Arrhenius plot introduces interpretive complications. In the past, an equilibrium between enzyme forms has generally been posited in explanation (e.g., Rajender et al., 1970; Wedler et al., 1975), and in the case of chymotrypsin there is evidence to support such a hypothesis. The binding of inhibitors and substrates to α-chymotrypsin and to covalently modified forms of this enzyme show distinct deviations from linearity in van't Hoff plots (Schultz et al., 1977, 1979), and a structural transition of α-chymotrypsin under experimental conditions similar to those used in our own kinetic studies (Baggott & Klapper, 1976) has been reported (Kim & Lumry, 1971; Lumry & Biltonen, 1979). Nonetheless, there is reason to consider the remaining three models as well. From our general knowledge of chemical reactions it is unlikely that $A\!H^{\ddagger}$ would be temperature independent, although apparent independence may hold over the small temperature range to which most enzyme studies are limited. On the basis of the proton inventory technique (Schowen, 1977) the serine proteases may be capable of catalyzing reactions by more than one pathway, involving either a single proton or a cooperative multiple proton mechanism. Finally, a tetrahedral reaction intermediate has been commonly assumed as an obligatory step in serine protease catalysis (Bender & Kilheffer, 1973). O'Leary & Kluetz (1972) have proposed a pH-dependent change in rate-limiting

† From the Department of Chemistry, The Ohio State University, Columbus, Ohio 43210. *Received July 30, 1980.*

0006-2960/81/0420-1401$01.25/0

step to and from a tetrahedral intermediate to explain an observed ^{15}N kinetic isotope effect associated with α-chymotrypsin acylation, and we have proposed an obligatory intermediate in the deacylation of α-chymotrypsin to explain a time-dependent ^{18}O kinetic isotope effect (Wang et al., 1980).

We have undertaken a more detailed reexamination of the α-chymotrypsin case for a number of reasons. First, since nonlinear Arrhenius plots are observed for other enzyme-catalyzed reactions, it is instructive to characterize this phenomenon carefully. Second, any theory which purports to explain the catalytic ability of an enzyme must be able to predict the activation parameters $\Delta H^{\ddagger}$ and $\Delta S^{\ddagger}$. But when more complicated kinetic schemes, such as proposed in models ii through iv, apply, then the experimental results must be manipulated to extract the pertinent activation parameters, requiring knowledge of the correct scheme. Third, Inward & Jencks (1965) have studied the alcoholysis of α-chymotrypsinyl 2-furoate, Cht-F,[1] with a variety of alcohols. Based in part on the observed lack of correlation between reaction rate and alcohol pK_a, they concluded that alcohols cannot undergo unassisted reaction with the acyl-enzyme. However, their studies were carried out at 25 °C, a temperature within the range of the Arrhenius plot nonlinearity for hydrolysis of the acyl-enzyme (Baggott & Klapper, 1976). Were the transesterification reactions also nonlinear, then lack of correlation could arise from an extraneous factor. Finally, the temperature dependence of chymotrypsin-catalyzed reactions above 0 °C has been utilized for linear extrapolation to the low temperatures of cryoenzymology studies. This extrapolation has in turn been cited as evidence that a mechanism based on very low temperature studies is pertinent to the enzyme reaction carried out under more physiological conditions (e.g., Fink, 1977). The validity of this argument requires careful evaluation of the enzyme temperature dependence.

We report here on the reinvestigation of Cht-F, and Cht-PF hydrolyses. The new data confirm our original observations and are used to eliminate some simple explanations for the nonlinear Arrhenius curves. In addition, we have investigated the alcoholysis reactions of Inward & Jencks (1965). With each alcohol nonlinear Arrhenius plots are observed.

Methods and Materials

Three different procedures were utilized to measure α-chymotrypsin (Worthington Biochemicals Corp., lots CDI2LX or CDS) activity. The first of these was a slight modification of the single turnover procedure described elsewhere (Baggott & Klapper, 1976). Stock enzyme (100 mg in 10 mL of 10^{-3} M HCl stored at 5 °C) was diluted into aqueous buffer solution to a final concentration of 6–60 μM in a quartz cuvette with a 1-cm light path. For start of the reaction, the substrate *p*-nitrophenyl-2-(5-*n*-alkyl)furoate dissolved in acetonitrile was added to a concentration less than that of the enzyme. When the absorbance at 347 nm became constant, indicating total reaction of substrate, the first-order enzyme deacylation reaction was monitored at 245 nm. The temperature of the reaction mixture was monitored throughout the run, and in no case was a fluctuation of 0.1 °C exceeded. The voltage output from the Cary 16 spectrometer was recorded on a Heath strip-chart recorder determined to be accurate to approximately 0.5%. The data were fit to

$$A_t = A_\infty - \Delta A e^{-kt} \quad (1)$$

where the symbols have their usual meaning.

Since the spectra of the ester products and acyl-enzyme are so similar, a steady state rather than single turnover procedure was used to monitor transesterification reactions. Buffer solution containing alcohol was equilibrated in the spectrophotometer cell. Substrate was added to a final concentration >20 μM, and the apparently linear nonenzymatic release of *p*-nitrophenolate monitored at 400 nm. Then enzyme was added (to a final concentration of typically 2 μM), and the solution was monitored at 400 nm through the initial *p*-nitrophenolate burst and the steady-state reaction. The burst magnitude, proportional to the enzyme active site concentration, was determined by extrapolating the linear nonenzymatic and steady-state portions of the reaction curve to the time of enzyme addition and measuring the difference, ΔA_{burst}. The rate constant for enzyme turnover, k_{app}, was calculated from

$$k_{app} = (R - R_0)/\Delta A_{burst} \quad (2)$$

where R and R_0 are the measured steady state and nonenzymatic rates expressed as change in absorbance per unit time. An advantage to the use of eq 2 is that the molar extinction coefficient for *p*-nitrophenolate, which varies slightly with varying alcohol concentration, need not be determined separately.

The third assay procedure, used only to verify the steady-state results, was based on analysis by gas–liquid chromatography. Substrate to a final concentration of 750 μM was added to 10 mL of solution containing enzyme (20 μM), alcohol, and buffer; in parallel control experiments enzyme was omitted. Aliquots were removed as a function of time, quenched into dilute HCl (0.6 M), and kept at 0 °C for no longer than 30 min. The acidified reaction mixture was injected into a Varian-Aerograph Model 2700 gas chromatograph containing a short, empty precolumn to trap the nonvolatile components and a 6-ft glass column packed with 100/120 mesh Gas-Chrom Q coated with 3% OV-225 (Applied Science Lab, State College, PA). Elution was conducted at flow rates of 30 mL/min He. In general, the injector temperature was 265 °C, the detector temperature 280 °C, with the column maintained at 130 °C for 16 min and then raised to 180 °C at 24 °C/min. With this flow rate ethyl 2-(5-*n*-propyl)furoate was eluted at 170 °C with a retention time of 3.0 min, and 5-*n*-propylfuroic acid with a retention time of 9.4 min. The amounts of ester and acid injected were obtained by cutting and weighing the peaks from the strip-chart recorder paper. Peak weights were standardized by using known amounts of material.

All nonlinear data fitting was done by using algorithms based on either the GRIDLS or CURFIT subroutines of Bevington (1969). For the more complicated cases the fitting procedure was repeated by using different initial parameter estimates to ensure global minimization. The multiple linear regression analysis used was based on the subroutine REGRES from the same source.

The *p*-nitrophenyl esters of furoic and 5-*n*-propylfuroic acids were synthesized as described previously (Baggott & Klapper, 1976). Ethyl 2-(5-*n*-propyl)furoate was synthesized by refluxing a solution of the acid in concentrated HCl (3.0 mL) and absolute ethanol (50 mL) for 4–6 days. The product solution was diluted into 200 mL of H_2O, neutralized with Na_2CO_3, and extracted with ether 3 times. The pale yellow liquid obtained after evaporation of the ether and excess alcohol was judged pure on the basis of gas chromatography and was identified by its mass spectrum. All other compounds were purchased commerically and used with no further purification, except for the alcohols which were redistilled, and *p*-nitro-

[1] Abbreviations used: Cht-F, α-chymotrypsinyl 2-furoate; Cht-PF, α-chymotrypsinyl 2-(5-*n*-propyl)furoate; Cht-MF, α-chymotrypsinyl 2-(5-methyl)furoate; Cht-BF, α-chymotrypsinyl 2-(5-*n*-butyl)furoate; GLC, gas–liquid chromatography.

Table I: Models Tested as Explanations for the Cht-PF Results of Figure 1

model	reactions	apparent rate constant	adjustable parameters	χ^2[a]
I	$EA' \overset{K}{\rightleftharpoons} EA \xrightarrow{k} E + P$	$k_{app} = kK/(1+K)$	$\Delta H^{\ddagger}, \Delta S^{\ddagger}, \Delta H, \Delta S$	496.7
II	$EA \xrightarrow{k_1} E + P$; $EA \xrightarrow{k_2} E + P$	$k_{app} = k_1 + k_2$	$\Delta H_1^{\ddagger}, \Delta S_1^{\ddagger}, \Delta H_2^{\ddagger}, \Delta S_2^{\ddagger}$	1232
III	$EA \rightarrow E + A$; $\Delta C_p^{\ddagger} = a + bT$		$\Delta H^{\circ}, \Delta S^{\circ}, a, b$	59.2
IV	$EA \xrightarrow{k_1} E + P$; $EA' \xrightarrow{k_2} E' + P$	$k_{app} = \alpha k_1 + (1-\alpha)k_2$	$\Delta H_1^{\ddagger}, \Delta S_1^{\ddagger}, \Delta H_2^{\ddagger}, \Delta S_2^{\ddagger}, \alpha$	190.9
V	$EA \rightarrow E + A$; $\Delta C_p^{\ddagger} = a + bT + cT^2$		$\Delta H^{\circ}, \Delta S^{\circ}, a, b, c$	62.2
Va	$EA \rightarrow E + A$; $\Delta C_p^{\ddagger} = a + bT + cT^{-2}$		$\Delta H^{\circ}, \Delta S^{\circ}, a, b, c$	129.7
VI	$EA \overset{K_1}{\rightleftharpoons} X_1 \overset{K_2}{\rightleftharpoons} X_2 \xrightarrow{k} E + P$	$k_{app} = kK_1K_2/(1 + K_1 + K_1K_2)$	$\Delta H_1, \Delta S_1, \Delta H_2, \Delta S_2, \Delta H^{\ddagger}, \Delta S^{\ddagger}$	410.1
VII	$EA \xrightarrow{k_1} E + P$; $K \Vert$; $EA' \xrightarrow{k_2} E + P$	$k_{app} = (k_1 + k_2K)/(1 + K)$	$\Delta H, \Delta S, \Delta H_1^{\ddagger}, \Delta S_1^{\ddagger}, \Delta H_2^{\ddagger}, \Delta S_2^{\ddagger}$	23.2

[a] χ^2 is the sum of the residuals squared divided by the number of degrees of freedom, and was obtained from the nonlinear least-squares fit of each model to the Cht-PF data of Figure 1.

phenol which was recrystallized from 95% ethanol.

Results

A minimal scheme to represent the α-chymotrypsin-catalyzed reactions of esters (Bender & Kilheffer, 1973) is given by eq 3a,b, with EOH the enzyme and its active site serine

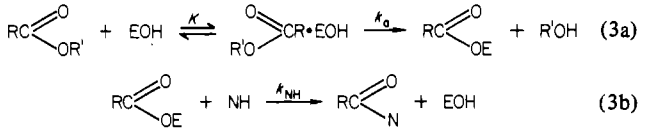

hydroxyl, and the reactant NH one of many possible nucleophiles. With esters in general, and especially with *p*-nitrophenyl esters, reaction 3a is faster than 3b. Thus, k_{NH} can be determined from the pseudo-first-order deacylation reaction which occurs under single-turnover conditions when the relative concentrations of reactants are NH $\gg$ EOH $\geq$ RCOOR^1 $\gg$ K_m. We have previously described the experimental protocol for obtaining k_{H_2O} (reaction 3b) of α-chymotrypsinyl 2-(5-*n*-alkyl)furoates (Baggott & Klapper, 1976). At that time we reported that Arrhenius plots of k_{H_2O} for Cht-F and Cht-PF deviated from linearity, a deviation we arbitrarily represented with two straight lines of different slope meeting at a discontinuity. These experiments have now been repeated. While the new results, obtained with greater care, are similar to those reported earlier, the curves display no apparent discontinuities (Figure 1).

As discussed in the introduction, the numerous explanations for a nonlinear Arrhenius plot can be grouped into four general categories. We have tested eight reaction models from three of these categories. Each model generates a different function for the temperature dependence of k_{H_2O} (Table I). After the theoretical function was fitted against the observed Cht-PF

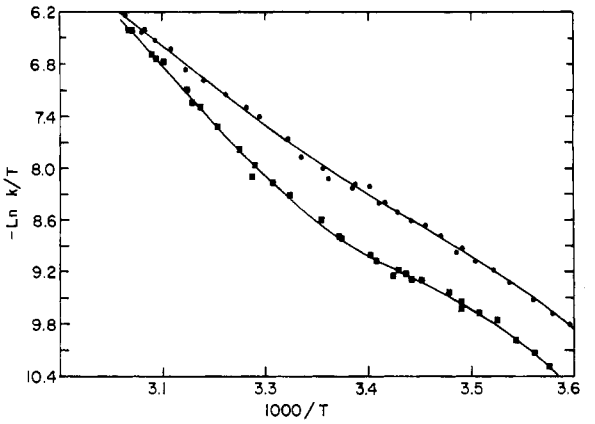

FIGURE 1: Temperature dependence of acyl-α-chymotrypsin hydrolysis (units of temperature, K, and of the first-order hydrolysis rate constant, min^{-1}). The rate constants were determined by the single turnover procedure described under Materials and Methods. All reactions were run in 0.2 M phosphate, pH 8.5. The solid lines were computed from the best fit analysis based on model VII (eq 6). (●) hydrolysis of Cht-F; (■) hydrolysis of Cht-PF.

results with an unconstrained, nonlinear least-squares minimization, a model's suitability was examined in two ways: first by the magnitude of χ^2 (Table I) and second by the presence of systematic deviations in a plot of residuals (Figure 2). On the basis of both criteria, the most appropriate of the tested models is number VII—a rapid, temperature-dependent equilibrium between two acyl-enzyme forms of differing reactivity. We could not test by direct fit the case of an obligatory kinetic intermediate with a temperature-dependent change in the rate-limiting step, because of the manner in which the rate constants were obtained. However, this mechanism would require that near the temperature of the

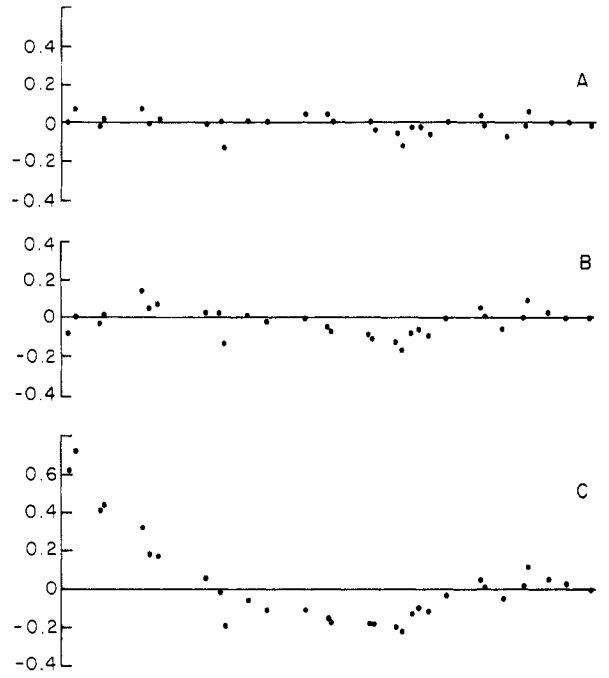

FIGURE 2: Example residuals plots from the fitting of experimental results to the hypothetical models of Table I. The residuals are expressed as $(k_{calcd} - k_{obsd})/k_{calcd}$, where k_{obsd} are the Cht-PF results of Figure 1 and are plotted against $1/T$(K). (A) Model VII; (B) model V; (C) Model VI.

Table II: Dependence of Cht-PF Deacylation on Enzyme Concentration[a]

enzyme (μM)	substrate (μM)	k_{H_2O} (min^{-1})[b]
6	6	0.0436 (0.0009)
20	20	0.0411 (0.0011)
40	40	0.0453 (0.0015)
60	60	0.0465 (0.0012)
60	30	0.0407 (0.0009)
60	10	0.0477 (0.0010)
		av 0.0443 (0.0029)

[a] All reactions were run in 0.2 M phosphate buffer adjusted to pH 8.5 at a temperature of 22 °C. [b] Individual constants were determined by a nonweighted, nonlinear regression analysis. Values in parentheses are the estimated standard deviations obtained from the fitting. The average of the six rate constants is weighted on the basis of the estimated individual standard deviations.

kinetic switch the observed deacylation should be a composite of at least two first-order processes. At every temperature investigated enzyme deacylation was a simple first-order reaction. Other models with complexity greater than that of VII might also fit the Cht-PF data adequately. However, the data are not of sufficient quality to warrant the serious consideration of more complex mechanisms. We propose that model VII is currently the best explanation of the Cht-PF results on the basis of parsimony. It should be noted that model IV results in a particularly poor fit of experimental results. This suggests that the nonlinearity cannot be explained in terms of chymotrypsin isozymes, or of a contaminating hydrolytic activity.

The nature of the two postulated Cht-PF species cannot be deduced from kinetic results alone. However, it can be shown that the equilibrium is not a protein aggregation. The hydrolysis rate constant was measured at different enzyme concentrations with the temperature set at 22 °C, the center of the proposed transition. No systematic variation of k_{H_2O} was observed under conditions such that either almost all the

Table III: Best-Fit Thermodynamic Variables for the Model of Two Enzyme Forms in a Rapid, Temperature-Dependent Equilibrium[a]

	Cht-PF	Cht-F
ΔH	33.6 (0.44)	*b*
ΔS	118 (1.5)	
$\Delta H_1^{\ddagger}$	29.3 (1.4)	19.0 (0.13)
$\Delta S_1^{\ddagger}$	−29.6 (1.4)	−7.78 (0.41)
$\Delta H_2^{\ddagger}$	28.1 (0.21)	19.4 (0.23)
$\Delta S_2^{\ddagger}$	−20.8 (0.66)	−5.08 (0.66)

[a] The equation $k_{app} = (k_1 + k_2K)/(1 + K)$ was cast into its explicit temperature-dependent form by substitution with $K = \exp(-\Delta H/RT + \Delta S/R)$, and $k_i = (\kappa T/h) \exp[(-\Delta H_i^{\ddagger}/RT) + (\Delta S_i^{\ddagger}/R)]$, $i = 1, 2$. The equation was then fit against the experimental results using the GRIDLS subroutine of Bevington (1969). Enthalpies are given in the units of kcal mol^{-1}, entropies in the units cal mol^{-1} deg^{-1}. Estimated standard deviations are presented in parentheses. [b] The Cht-F results were fit assuming the ΔH and ΔS obtained with the Cht-PF fit and allowing only the four activation parameters to vary.

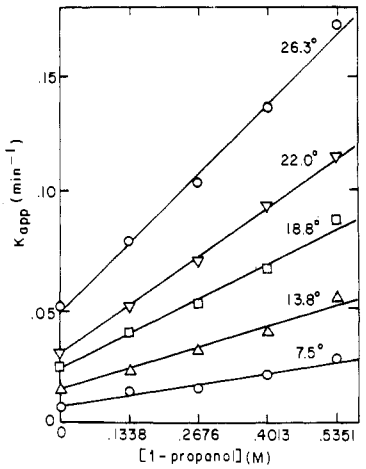

FIGURE 3: Reaction of Cht-PF with propanol; dependence on temperature and alcohol concentration.

enzyme was intially acylated or only a fraction of it was (Table II). Hence, neither self-association between Cht-PF molecules nor heterologous association between Cht-PF and free enzyme can explain the kinetic results, regardless of whether aggregation does or does not occur.

Fitting the Cht-F hydrolysis constants was not useful for discrimination between models. Apparently, the experimental uncertainties are too large to extract the relevant information from the Cht-F Arrhenius curvature, which is shallower than that of Cht-PF (Figure 1). Hence, the Cht-F data were fit to the equation of model VII, with the assumption that the equilibrium between acyl-enzyme forms is identical for Cht-F and Cht-PF. The thermodynamic and kinetic variables obtained from the fits to model VII are given in Table III.

Were the proposed model correct, then nonlinear Arrhenius plots should be an inherent property of the acyl-enzyme, and should be observed with nucleophiles other than water. We, therefore turned our attention to chymotrypsin-catalyzed transesterifications. The single turnover protocol used in the hydrolysis studies relies on a spectral difference between the furoate product and furoyl-enzyme ester. Since the product of an alcoholysis is also an ester, this procedure could not be used for a reliable determination of k_{ROH}, and a steady-state assay in which *p*-nitrophenolate release is monitored was substituted. The rate constant obtained is linearly dependent on alcohol up to the highest concentrations of all the alcohols tested (Inward & Jencks, 1965); an example is presented in Figure 3. The intercept of the straight line is the hydrolysis

Table IV: Comparison of Measurement Techniques[a]

technique	k_{H_2O} (min^{-1})	$k_{CH_3CH_2OH}$ (min^{-1} M)
single turnover	0.0421 (0.0015)	
steady state-spectrophotometric	0.040	0.080 (0.002)
steady-state-GLC	0.055 (0.008)	0.078 (0.005)

[a] All rate constants refer to the hydrolysis or ethanolysis of α-chymotrypsinyl 2-(5-*n*-propyl)furoate. The three techniques of measurement are described under Materials and Methods. All reactions were run at 23 °C. In the single turnover experiment the pH was 8.5; in the other two, 9.0. In the steady-state spectrophotometric assay, k_{H_2O} was measured in the absence of alcohol; $k_{CH_3CH_2OH}$ was obtained from the slope of the k_{app} vs. CH_3CH_2OH concentration. In the gas–liquid chromatography assay, the reaction was run in a 3% (v/v) ethanol concentration and the rate constants were measured from the time dependence of acid and ester products released. In all cases the initial substrate was *p*-nitrophenyl 2-(5-*n*-propyl)furoate. Estimated standard deviations are given in parentheses.

rate constant, k_{H_2O}, as seen by the coincidence of the measured k_{H_2O} with the intercept. Thus, in aqueous alcohol solutions the acylated enzyme undergoes hydrolysis and alcoholysis simultaneously, and the measured pseudo-first-order rate constant is the sum

$$k_{app} = k_{H_2O} + k_{ROH}(ROH) \quad (4)$$

The observed linearity requires either that Cht-PF and alcohol form no enzyme–substrate complex or that the alcohol K_M is greater than the highest concentration used in every case. The slope of each straight line in Figure 3 is k_{ROH}, provided hydrolysis is unaffected by the added alcohol. For verification of this in at least one case, both the ester and acid products formed during the simultaneous hydrolysis and ethanolysis of Cht-PF were measured after separation by gas–liquid chromatography. As detected by GLC, the production of both was linear with time, and the rate constants obtained were similar to those determined by the spectrophotometric steady state procedure. The results obtained with a 3% (v/v) ethanol solution at 23 °C are presented in Table IV. At higher ethanol concentrations transesterification so outweighs hydrolysis that only k_{ROH} can be determined by the GLC method. At 7 °C k_{app} (determined spectrophotometrically) increases linearly with ethanol concentration up to 15% (v/v). At this highest alcohol concentration k_{ROH} is the same whether obtained by the GLC method or from the slope of the k_{app} vs. ethanol concentration curve. We therefore concluded that k_{H_2O} is unaffected by the alcohol, and we routinely determined k_{ROH} by the steady-state spectrophotometric procedure.

The K_M of *p*-nitrophenyl 2-(5-*n*-propyl)furoate, the reaction substrate, increases at higher alcohol concentrations. For example, K_M was estimated as 0.7 μM and 2 μM at 9.7 and 42.0 °C, respectively, with no alcohol present. In a 15% (v/v) ethanol solution the K_M rose to 1.7 μM and ~4 μM at the same two temperatures. Since all reactions were run routinely with substrate >20 μM, the effect of alcohols on substrate K_M was assumed to be negligible.

Cht-PF hydrolysis has a pH dependence which can be described in terms of a single proton acid/base equilibrium with a pK_a near 7 (Baggott & Klapper, 1976). The second-order ethanolysis constant has a similar pH dependence (Figure 4; pH measured after the addition of ethanol). The pK_a's determined at 20 °C were 7.01 (0.08) and 7.06 (0.06) in water and 25% (v/v) aqueous ethanol, respectively. We have concluded that (i) k_{ROH} measured at pH 9.0 is a good approximation to the pH-independent alcoholysis constant and (ii)

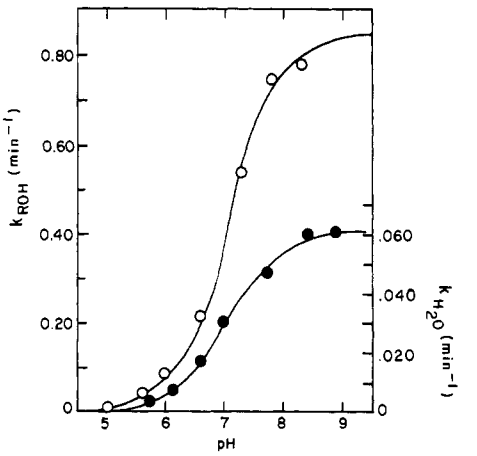

FIGURE 4: α-Chymotrypsin pH–rate profile. Rate constants were determined by the steady-state spectrophotometric method described under Materials and Methods. Measurements were made at 20 °C in 0.1 M Na_2HPO_4–0.025 M $Na_3B_4O_7$. When used, ethanol was added to a final concentration of 25% (v/v), and the pH adjusted in the presence of the alcohol. The substrate was *p*-nitrophenyl 2-(5-*n*-propyl)furoate. (●) Hydrolysis; (○) ethanol transesterification.

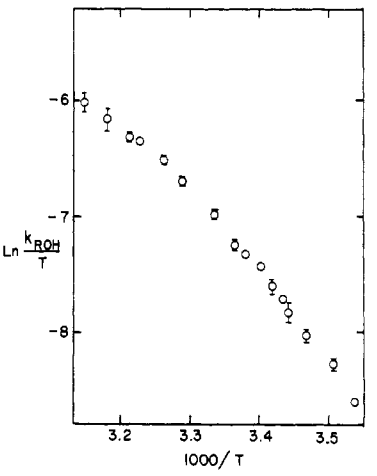

FIGURE 5: Temperature dependence of Cht-PF methanolysis. Conditions are those of Figure 4 except that the pH is maintained at 9.0, and the temperature is varied. (units of temperature, K, of the second-order rate constants, M^{-1} min^{-1}. Estimated standard deviations are indicated by the bars.

there is no significant shift in the reactivity pK_a over the alcohol concentrations used in the determination of k_{ROH}. All temperature-dependent studies were, therefore, carried out in 0.1 M Na_2HPO_4–0.025 M $Na_3B_4O_7$, with pH adjusted to 9.0 after the addition of alcohol.

The temperature dependence of k_{ROH} was determined for the reaction of Cht-PF with 10 alcohols listed in Table V. The results for the methanolysis of Cht-PF (Figure 5) are typical. With every alcohol we obtained a nonlinear Arrhenius plot, which was concave down between 20 and 30 °C. The data for each alcohol were fit assuming model VII and assigning to the equilibrium enthalpy and entropy the values obtained from the Cht-PF hydrolysis results (Table III). Thus, only the four activation parameters were permitted to vary with no constraint. With each alcohol there was good correspondence between observed and best fit calculated results, as judged by the absence of systematic deviations in residuals plots. These results support the validity of model VII. The high-temperature activation parameters obtained in these fittings are collected in Table V. (The low-temperature parameters were obtained with unsatisfactorily large standard deviations, due to the small number of points below 15 °C.)

Table V: Activation Parameters for the Alcoholysis of Cht-PF[a]

alcohol	$\Delta H^{\ddagger}$ (kcal mol^{-1})	$\Delta S^{\ddagger}$ (cal mol^{-1} deg^{-1})	$k^{30\,°C}_{calcd}$[c] (M min^{-1})	σ^*[d]	V[e] (Å^3)
1, methanol	10.9 (0.13)[b]	−32.6 (0.45)[b]	1.18×10^{-3}	0.49	36.1
2, ethanol	6.7 (0.43)	−49.0 (1.42)	0.385×10^{-3}	0.0	53.1
3, propanol	10.0 (0.19)	−36.1 (0.61)	0.955×10^{-3}	−0.10	70.1
4, butanol	10.2 (0.37)	−33.8 (1.22)	2.18×10^{-3}	−0.115	87.1
5, pentanol	11.2 (0.92)	−29.2 (3.00)	4.45×10^{-3}	−0.13	104.1
6, hexanol	13.9 (0.72)	−19.5 (2.35)	6.86×10^{-3}	−0.14	121.1
7, methoxyethanol	7.4 (0.58)	−44.2 (1.92)	1.26×10^{-3}	0.52	76.3
8, propargyl alcohol	6.5 (0.23)	−44.0 (0.76)	5.95×10^{-3}	1.64	62.9
9, chlorethanol	9.6 (0.48)	−36.4 (1.57)	1.90×10^{-3}	1.05	67.2
10, dichloroethanol	12.1 (1.58)	−27.2 (5.14)	2.86×10^{-3}	2.13	104.1

[a] $\Delta H^{\ddagger}$ and $\Delta S^{\ddagger}$ were obtained by fitting rate constants to the equation for model VII in Table I. The equilibrium ethalpy and entropy were assigned as 33.6 kcal mol^{-1} and 118 cal mol^{-1} deg^{-1} (Table II). The activation parameters given are those for the higher temperature form of Cht-PF. Due to the paucity of data below 15 °C, the activation parameters for the lower temperature form have unacceptably large estimated standard deviations and were, therefore, not included. [b] The figures given in parentheses are estimated standard deviations. [c] The rate constant calculated by the equation $k = (\kappa T/h) \exp[-\Delta H^{\ddagger}/RT + \Delta S^{\ddagger}/R]$. [d] Obtained from Wells (1963). [e] Volumes were calculated from the incremental atomic volumes collected by Edward (1970).

Discussion

The rate constants for the hydrolysis of Cht-F and Cht-PF (Figure 1) are similar to those reported earlier (Baggott & Klapper, 1976) and support our original observation of nonlinear Arrhenius curves for these two reactions. An analysis of the Cht-PF hydrolysis results suggests that the simplest explanation of this nonlinearity is the assumption of a temperature-dependent equilibrium between two acyl-enzyme forms which hydrolyze with different reactivities and with rates slower than their interconversion (eq 5).

$$\begin{array}{ccc} EA & \xrightarrow{k_1} & E + \text{product} \\ \kappa \downarrow\uparrow & & \\ EA' & \xrightarrow{k_2} & E + \text{product} \end{array} \qquad (5)$$

The nature of the two enzyme species cannot be deduced from the kinetic results we have obtained, although protein aggregation has been eliminated from consideration. α-Chymotrypsin is known to undergo an alkaline transition [e.g., McConn et al. (1969) and Kim & Lumry (1971)] with a controlling pK_a, between 8.5 and 9, near to the pH of our experiments. However, it has been reported that this transition is not observed when the active-site serine is blocked with an acetyl (Lumry & Biltonen, 1969) and diisopropylphosphoryl (McConn et al., 1969) group and that with substrate or inhibitor bound to the enzyme the pK_a controlling the transition shifts to greater than 10 (McConn et al., 1968; Wedler & Bender, 1969). Moreover, it has been proposed that the alkaline form of the enzyme is inactive (McConn et al., 1969; Fersht & Requena, 1971). These reported properties are not consistent with the equilibrium proposed here. Rossi & Bernhard (1971) have found that the rates of urea or sodium dodecyl sulfate induced α-chymotrypsin denaturation are 2–3 orders of magnitude faster than the similar denaturation of α-chymotrypsin acylated with the indoleacryloyl group. This observation suggests that the acylated and free enzymes may have different conformations. Thus, a relationship between the two species equilibrium postulated here and the alkaline transition of the free enzyme is problematic.

Assuming the scheme of eq 5 and using the best fit values of the six thermodynamic and activation constants (Table III) it is possible to compute the fraction of Cht-PF in the high- or low-temperature form and the fraction of the total product released via one or the other (see footnote *a*, Table III). The results are plotted vs. temperature in Figure 6. That the curve for the fraction of Cht-PF in the high-temperature form lies at lower temperatures than the curve for the fraction of product

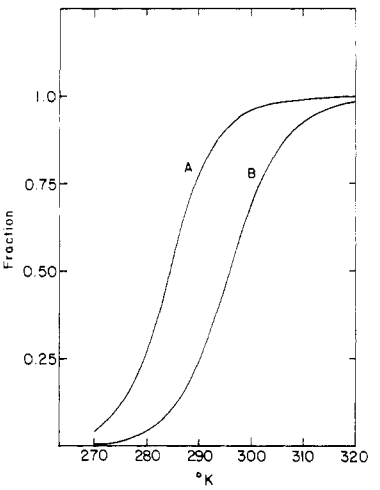

FIGURE 6: (A) Fraction of Cht-PF in the high temperature form; (B) fraction of 2-(5-*n*-propyl)furoate production which proceeds through the high temperature form of Cht-PF. Curve A is calculated from the temperature dependence of the acyl-enzyme equilibrium using the ΔH and ΔS given in Table III. Curve B represents the temperature dependence for that fraction of the product which is formed via the high-temperature acyl-enzyme species and is calculated from $fk_1/[fk_1 + (1-f)k_2]$, where f is the fraction of enzyme in the high-temperature form, and k_1, k_2 are the high- and low-temperature rate constants, respectively.

released through that form indicates the greater reactivity (after temperature normalization) of the low-temperature species. The shape of the Arrhenius curve for the Cht-PF hydrolysis—concave up between 20 and 30 °C—suggests the same. Qualitatively similar results are obtained with Cht-F. The structural basis of the observed reactivity differences is not known. It is, however, interesting to note that, with both Cht-PF and Cht-F, the greater reactivity at lower temperatures is due to an increase in $\Delta S^{\ddagger}$; activation enthalpies at low and high temperatures are the same within experimental error (Table III). This suggests that reactivity differences may be due solely to a change in geometric substrate–enzyme relationships.

Arrhenius plots for the hydrolyses of Cht-MF and Cht-BF are linear (Baggott & Klapper, 1976). Thus, in these cases the high- and low-temperature species must have closely similar reactivities. With Cht-F and Cht-PF, the low-temperature form is approximately 2- and 10-fold more reactive, respectively. We have not been able to obtain reliable rate constants for the reaction of alcohols with the Cht-PF low-temperature form. However, the shapes of the Arrhenius plots—concave

down between 20 and 30 °C for all alcohols used—suggest that this species has the lesser reactivity in transesterification, opposite to the hydrolysis results. Thus, the relative reactivities of high- and low-temperature acyl-enzyme species vary both quantitatively and qualitatively dependent upon the reactants, even though (i) the site of covalent attachment between acyl group and enzyme is invariant, (ii) the reaction mechanism is most probably the same irrespective of substrate, and (iii) experimental results suggest that alcohol (this paper) and water (Tanizawa & Bender, 1974) may not form a substrate complex with acyl-enzyme.

Inward & Jencks (1965), who previously studied the reaction of Cht-F with various alcohols at 25 °C, found no linear correlation between ln k_{ROH} and the alcohol pK_a. Before conclusions can be drawn from this type of analysis, the contribution of the acyl-enzyme equilibrium to the net rate must be eliminated. When this is done by computing hypothetical rate constants with the high-temperature activation parameters in Table V, there is still no linear correlation with pK_a. It is almost a truism that linear-free-energy relationships are not applicable to enzyme-catalyzed reactions because of specific geometric interactions between enzymes and their substrates [e.g., Bruice & Benkovic (1966)]. Because we could find no evidence for the specific binding of alcohols to Cht-PF (deacylation increased linearly with alcohol concentration to the highest levels examined), we were not surprised to find that the corrected rate constants do obey a linear relationship defined by

$$\ln k_{ROH} = \ln k^0_{ROH} + \rho\sigma^* + \delta V \qquad (6)$$

where V is the volume of the alcohol as defined by Edward (1970), σ^* the alcohol's Taft polarity constant (an energy measure equivalent to, but more fundamental than pK_a), δ and ρ their respective proportionality constants, and k^0_{ROH} the rate constant for the hypothetical alcohol with the reactivity of ethanol but with no volume. For the corrected rate constants calculated at 30 °C the linear best fit to eq 6 yields ln k^0_{ROH} = −6.5 ± 0.90, ρ = 1.0 ± 0.36, and δ = 0.021 ± 0.010, with a multiple linear correlation coefficient of 0.90.

The standard deviations associated with ρ and δ are large, and, thus, a detailed discussion of their mechanistic implications is not warranted. However, the value of ρ is sufficiently positive to suggest that electron-withdrawing substituents on the alcohol moiety serve to stabilize either a rate-limiting transition state, or a reaction intermediate, in which there may be an expression of partial negative charge. The dependence of the rate constant on alcohol volume has a less obvious interpretation. One of us has previously proposed that rate enhancement specificity in enzyme-catalyzed reactions may be controlled in part by the durospatial effect (Klapper, 1973); rate acceleration is effected by relieving steric enzyme–substrate interactions as the reaction proceeds through the transition state. Since this is largely a geometric interaction (bond angle and distance distortions need not be introduced), the durospatial effect in apolar compounds should be observed experimentally as a volume contribution over a homologous series, and should also be reflected in the entropy of activation. Previous results obtained with homologous series of acids suggested that the durospatial effect may be operative in chymotrypsin (Baggott & Klapper, 1976). It is interesting to note, therefore, that there is also a linear correlation between ΔS^* and alcohol volume (Figure 7). For this reason we propose that the durospatial effect may be an important contributor to the rate of chymotrypsin-catalyzed transesterifications.

In summary, we have verified our original observation that

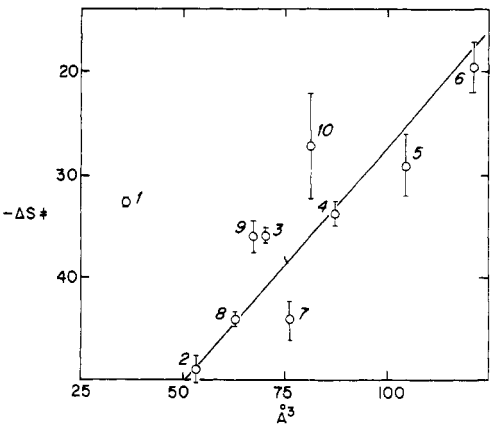

FIGURE 7: Linear correlation between ΔS^* and alcohol volume. Activation entropies for Cht-PF transesterification and alcohol volumes taken from Table V. Estimated standard deviations are given by the brackets. Alcohols are numbered in the same order as listed in Table V. The straight line has been entered arbitrarily. By linear least squares (methanol omitted), ΔS^* = −66.5 (2.2) + 0.393 (0.030) V, with the correlation coefficient r = 0.86.

α-chymotrypsin catalysis of ester hydrolysis can display nonlinear Arrhenius plots and have extended this observation to transesterification reactions as well. We propose that this nonlinearity is most simply explained in terms of a structural transition between two acyl-enzyme forms whose reactivity difference may lay solely in differences of activation entropy. Some other, but not all, possible explanations have been ruled out by fitting kinetic data to models. Finally, the transesterification results may be interpreted qualitatively in terms both of the electron-withdrawing propensities of substituents on the alcohol and on a durospatial effect between alcohol and enzyme.

Acknowledgments

We are indebted to the Instruction and Research Computer Center of The Ohio State University for free time provided to us on an Amdahl 470.

References

Baggott, J. E., & Klapper, M. H. (1976) *Biochemistry 15*, 1473.

Bender, M. L., & Kilheffer, J. V. (1973) *CRC Crit. Rev. Biochem. 1*, 149.

Bevington, P. R. (1969) *Data Reduction and Error Analysis for the Physical Sciences*, McGraw-Hill, New York.

Bruice, T. C., & Benkovic, S. J. (1966) *Bioorganic Mechanisms*, Vol. 1, W. A. Benjamin, New York.

Edward, J. T. (1970) *J. Chem. Educ. 47*, 261.

Fersht, A. R., & Requena, Y. (1971) *J. Mol. Biol. 60*, 279.

Fink, A. L. (1977) *Acc. Chem. Res. 10*, 233.

Graves, D. J., Sealock, R. W., & Wang, J. H. (1965) *Biochemistry 4*, 290.

Helmreich, E., & Cori, C. F. (1964) *Proc. Natl. Acad. Sci. U.S.A. 52*, 647.

Inward, P. W., & Jencks, W. P. (1965) *J. Biol. Chem. 240*, 1986.

Kayne, F. J., & Suelter, C. H. (1965) *J. Am. Chem. Soc. 87*, 897.

Kim, Y. D., & Lumry, R. (1971) *J. Am. Chem. Soc. 93*, 1003.

Kistiakowsky, G. B., & Lumry, R. (1949) *J. Am. Chem. Soc. 71*, 2006.

Klapper, M. H. (1973) *Prog. Bioorg. Chem. 2*, 55.

Kosicki, G. W., & Srere, P. A. (1961) *J. Biol. Chem. 236*, 2560.

Lumry, R., & Biltonen, R. (1969) in *Structure and Stability of Biological Macromolecules* (Timasheff, S. N., & Fasman, G. D., Eds.) Vol. 2, pp 65–212, Marcel Dekker, New York.

Massey, V., Curti, B., & Ganther, H. (1966) *J. Biol. Chem. 241*, 2347.

Matheson, R. R., & Scheraga, H. A. (1979) *Biochemistry 18*, 2446.

McConn, J., Ku, E., Odell, C., Czerlinski, G., & Hess, G. P. (1968) *Science (Washington, D.C.) 161*, 274.

McConn, J., Fasman, G. D., & Hess, G. P. (1969) *J. Mol. Biol. 39*, 551.

O'Leary, M. H., & Kluetz, M. D. (1972) *J. Am. Chem. Soc. 94*, 3585.

Rajender, S., Han, M., & Lumry, R. (1970) *J. Am. Chem. Soc. 92*, 1378.

Rossi, G. L., & Bernhard, S. A. (1971) *J. Mol. Biol. 55*, 215.

Saint-Blancard, J., Clochard, A., Cozzone, P., Berthou, J., & Jolles, P. (1977) *Biochim. Biophys. Acta 491*, 354.

Schultz, R. M., Konovessi-Panayotatos, A., & Peters, J. R. (1977) *Biochemistry 16*, 2194.

Schultz, R. M., Varma-Nelson, P., Peters, J. R., & Treadway, W. J. (1979) *J. Biol. Chem. 254*, 12411.

Tanizawa, K., & Bender, M. L. (1974) *J. Biol. Chem. 249*, 2130.

Wang, C.-L. A., Trout, C. M., Calvo, K. C., Klapper, M. H., & Wong, L. K. (1980) *J. Am. Chem. Soc. 102*, 1221.

Wedler, F. C., & Bender, M. L. (1969) *J. Am. Chem. Soc. 91*, 3894.

Wedler, F. C., Uretsky, L. S., McClune, G., & Cencula, J. (1975) *Arch. Biochem. Biophys. 170*, 476.

Wells, P. R. (1963) *Chem. Rev. 63*, 171.